Int J Adv Manuf Technol (2011) 53:699–709
DOI 10.1007/s00170-010-2849-2

ORIGINAL ARTICLE

Generating tool-path with smooth posture change for five-axis sculptured surface machining based on cutter's accessibility map

L. L. Li · Y. F. Zhang · H. Y. Li · L. Geng

Received: 26 May 2009 / Accepted: 16 July 2010 / Published online: 4 August 2010

Abstract In five-axis high speed milling, one of the key requirements to ensure the quality of the machined surface is that the tool-path must be smooth, i.e., the cutter posture change from one cutter contact point to the next needs to be minimized. This paper presents a new method for generating five-axis tool-paths with smooth tool motion and high efficiency based on the accessibility map (A-map) of the cutter at a point on the part surface. The cutter's A-map at a point refers to its posture range in terms of the two rotational angles, within which the cutter does not have any interference with the part and the surrounding objects. By using the A-map at a point, the posture change rates along the possible cutting directions (called the smoothness map or S-map) at the point are estimated. Based on the A-maps and S-maps of all the sampled points of the part surface, the initial tool-path with the smoothest posture change is generated first. Subsequently, the adjacent tool-paths are generated one at a time by considering both path smoothness and machining efficiency. Compared with traditional tool-path generation methods, e.g., iso-planar, the proposed method can generate tool-paths with smaller posture change rate and yet shorter overall path length. The developed techniques can be used to automate five-axis tool-path generation, in particular for high speed machining (finish cut).

Keywords Five-axis milling · Tool-path generation · Cutter posture change · Machining strip width

L. L. Li · Y. F. Zhang (✉) · H. Y. Li · L. Geng
Department of Mechanical Engineering,
National University of Singapore,
10 Kent Ridge Crescent,
Singapore 119260, Singapore
e-mail: mpezyf@nus.edu.sg

1 Introduction

As the need for complex components such as three-dimensional (3D) moulds and dies has risen, sculptured surface machining has assumed a more and more important role in manufacturing for the last few decades. The employment of five-axis numerical control (NC) machines in sculptured surface machining offers numerous advantages over three-axis mode such as setup reduction, fast material removal rates, and improved surface quality. To make the best use of five-axis machining, however, problems related to complication and complexity caused by the two additional rotary axes have to be solved. One of the challenging tasks is to automatically generate error-free tool-path without user interaction for machining sculptured surfaces.

In the process planning of five-axis finish cut, the tool-path generation task is to select a tool-path pattern, generate the cutter contact (CC) points that satisfy the accuracy requirement, and determine the cutter's posture (orientation) at every CC point without causing any interference. During this process, to ensure the quality of the machined surface, the smooth dynamics of cutter motion is a must, i.e., the posture change from one point to the next must be minimized. Extreme change in cutter posture, which is necessary for interference avoidance, is a major cause for the unnatural movement of the cutter and will lead to over and under cutting in five-axis finish and undesirable irregularity of the surface appearance [1, 2]. So far, there is limited reported work on obtaining the cutter location (CL) data with smooth continuous change in cutter postures along a pre-set path and cutting direction [1–3], and there is no reported method that can generate CL data with global optimization of cutter motion dynamics with respect to a cutting direction in five-axis finish cut.

This paper presents a new optimization method aimed at obtaining CL data with smooth cutter dynamics and high cutting efficiency in five-axis tool-path generation. The method is based on two sets of information that characterize the potential cutting configurations of a cutter at a point on the part surface. The first one is the cutter's accessibility map (A-map) representing the interference-free posture ranges in terms of the two rotational angles. The second is the cutter's smoothness map (S-map) indicating the posture change rates along all possible cutting directions. Based on these two sets of information of all the sampled points of the surface, the initial tool-path with the smoothest posture change is generated. Subsequently, the adjacent paths are generated one at a time in an iterative manner by considering both cutting efficiency and cutter dynamics, until the whole surface is covered. The cutter considered in this paper is a cylindrical cutter with a fillet-end, which also covers the flat-end cutter and the ball-end cutter.

The remaining of this paper is organized as follows. Related work of tool-path generation and optimization is reviewed in Section 2, followed by a brief introduction on A-map evaluation and its application in optimal cutter selection in Section 3. Section 4 describes the concept of S-map and its evaluation method. In Section 5, the new method for tool-path generation in five-axis sculptured surface machining is presented. In Section 6, an example is given to show the effectiveness of the algorithm. Finally, conclusion remarks are given in Section 7.

2 Related works

During the last 20 years, much research work has been carried out in the area of automatic generation of interference-free and optimal tool-paths for the five-axis machining of freeform surfaces [4]. Many approaches have been proposed, including: (1) iso-planar approaches [5–7]; (2) iso-parametric approaches [8, 9]; and (3) constant-scallop approaches [10–13]. These methods generally start path planning from the part surface boundaries. Based on each cutter contact (CC) point on the current path, the next (adjacent) path is generated by considering the local surface geometry and cutting swept-envelope. Although surface geometry has been considered in these approaches, the consideration is usually limited to the local machining gouging avoidance with respect to a user-specified cutting direction.

Many efforts have been focused on generating tool-paths with high machining efficiency. The relationship between the cutting direction and the part surface geometry has been extensively studied for three-axis milling operations [14, 15]. For five-axis machining, Kruth and Klewais [16] suggested that at a point, in order to maximize the machining strip width, the path direction should match the principle curvature direction of the part surface at the point. Kim and Sarma [17] developed a greedy approach to generate the time-optimal tool-paths along directions of maximum kinematic performance. Chiou and Lee [18] presented a machining potential field method for the global optimization of tool-path direction by calculating the machining strip width. The optimal cutting direction is the one that produces the largest feasible machining strip width. Obviously, the above two methods aim at finding the cutting direction that produces the shortest overall tool-path. In five-axis machining, machining efficiency is certainly a very important factor to be considered in path planning, surface accuracy is, however, an equally important factor to be considered. Traditionally, surface accuracy is considered by limiting the scallop height between adjacent paths, the dynamics of the cutter motion, i.e., smoothness of tool-path is seldom considered. In reality, a highly smooth tool-path is a necessary condition to ensure machining accuracy in five-axis machining, especially in high speed mode.

With regard to dynamics of cutter motion in five-axis tool-path generation, some methods have been proposed to generate collision-free CL data with a smooth continuous change in tool posture. Morishige et al. [2] applied the concept of 3D C-space to construct a collision-free space (in terms of cutter orientation) along a path trajectory curve for the tool center. The optimal CL data on this path is then obtained by finding a continuous curve through the inside of the space. In Balasubramanium et al.'s approach [1] for tool-path generation, a heuristic was introduced to select the tool posture at a CC point from visibility data such that the orientation jump from the previous one is minimized. Wang and Tang [3] proposed an optimization algorithm to smooth the tool orientations in respect to a user-specified tool's angular velocity limit. In these approaches, CL data are optimized locally on the tool postures at the pre-determined cutter locations. On the other hand, some reported research efforts considered the effect of cutting force and tool deflection for tool-path generation. López et al. [19, 20] investigated the influence of cutting force and tool deflection on tool-path optimization. A methodology was presented for tool-path selection based on the calculation of the minimum cutting force component related to tool deflection. The orientation angle in five-axis machining is firstly selected, and then feeding direction by testing the value of the deflection force. In nature, this method focuses on the optimization of feeding direction, not the cutter's postures.

This paper presents an optimization approach for both cutter locations and postures in five-axis tool-path generation by considering interference avoidance, machining

efficiency, and in particular, smooth posture changes. Using the A-maps and S-maps at all the sampled points on the surface, the optimal tool-paths are generated such that the change in cutter posture is minimized when passing through the generated CC points. Besides, machining strip width between adjacent paths is also considered to achieve high machining efficiency.

3 The accessibility map of a cutter at a point

The accessibility map (A-map) is defined in respect to a cutter positioned at a point on the part surface. It refers to the posture range in terms of the two rotational angles, and within this range, the cutter does not have any interference with the part and the surrounding objects. The A-map effectively characterizes the accessibility of a cutter to a point, which provides important geometric information for cutter selection and interference-free tool-path generation. A brief introduction of A-map is given here.

As shown in Fig. 1a, the local frame ($X_L - Y_L - Z_L$) originates at the point of interest $\mathbf{P}_c$ with $\boldsymbol{Z}_L$-axis along the surface normal vector, $\boldsymbol{X}_L$-axis along the surface *maximum* principal direction, and $\boldsymbol{Y}_L$-axis along the surface *minimum* principal direction [21]. A cutter posture (λ, θ) means that the cutter's axis inclines counter-clockwise with λ about $\boldsymbol{Y}_L$-axis and rotates a θ about $\boldsymbol{Z}_L$-axis. The A-map of the cutter at this point is represented in [λ, θ] domain in the local frame. In order to find the A-map at the point, the four accessible posture ranges based on their respective interference-free attributes, i.e., machine axis limits (ML), local-gouging (LG), rear-gouging (RG), and global-collision (GC), are found first. For implementation, the part surface (to be machined) is firstly sampled into m points. At a specific point, the feasible range of θ–λ based on ML is first calculated. θ is then uniformly sampled into k angles. At each discrete θ, the minimum λ needed to eliminate LG is found. For RG and GC, the range of λ at each discrete θ that is interference-free from all the remaining $(m-1)$ points is identified. The A-map at this point is simply the intersection of these four accessible posture ranges (see Fig. 1b). The overall algorithm for finding the A-map for a cutter at a point on the part surface is called the cutter accessibility (CA) algorithm. Obviously, the CA algorithm is numerical in nature with a computational complexity of $O(km)$. For more details about the evaluation of the A-map, readers can refer to [22].

A direct application of this A-map concept is for the optimal cutter selection to finish a given sculptured surface [22]. By applying the CA algorithm to all the sampled points on a part surface, one can judge whether a cutter can traverse the whole surface without any interference. The optimal cutter can therefore be the largest available cutter with non-empty A-maps at all sampled surface points.

4 The smoothness map of a cutter at a point

Since the A-map only characterizes the geometric property of the cutter's potential configuration at a point, it is necessary to add the dynamic property of the cutter at the point to complete the information set. The dynamic property of cutter is a complex issue involving many factors, e.g., feed-rate, cutting load, and path smoothness. Since this work focuses on finishing tool-path planning, only path smoothness is considered, which is measured by the posture change rate (PCR) of the cutter at the point. Given a CC point $\mathbf{P}_i$ and next CC point $\mathbf{P}_{i+1}$ on a path, PCR_i is defined as:

$$PCR_i = \frac{|\mathbf{V}_{i+1} - \mathbf{V}_i|}{|\mathbf{P}_{i+1} - \mathbf{P}_i|} \tag{1}$$

Where $\mathbf{V}_i$ is the unit vector of cutter axis along its posture (θ_i, λ_i) at $\mathbf{P}_i$ in the global frame. Before a cutting direction is selected, it is necessary to obtain the PCRs along all possible cutting directions, which is called the smoothness

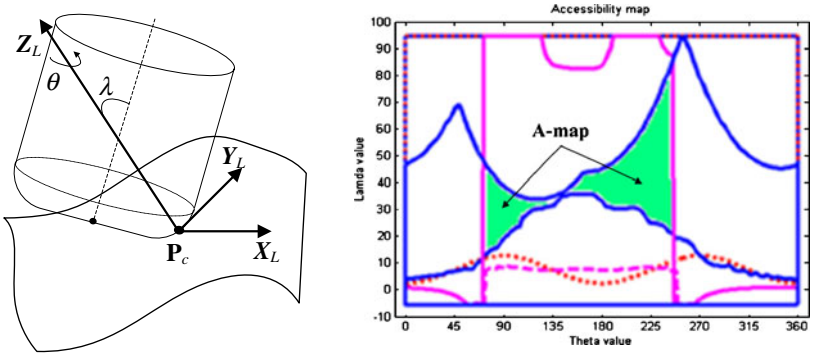

(a) The cutter in the local frame (b) The A-map at $\mathbf{P}_c$

Fig. 1 The cutter A-map at a point on the part surface. **a** The cutter in the local frame. **b** The A-map at $\mathbf{P}_c$

map (S-map) at the point. For implementation, the S-map at a point can be constructed by finding the PCRs of all the sampled discrete cutting directions. As shown in Fig. 2, the discrete cutting directions are specified in the ***X***–***Y*** plane of the global frame and by angle β_k from the ***X***-axis. By using β_k as the angular position and PCR_k as the radius, the S-map is constructed. At this point, the direction with the minimum PCR_k in the S-map is the optimal cutting direction.

To obtain PCR_k along one cutting direction β_k according to Eq. 1, two corresponding cutter postures at the current point and the next one need to be known. However, at this stage, these two postures are not finalized, only the A-maps at the sampled points are available. Therefore, PCR_k can only be estimated. In the following sections, we firstly present a time-efficient algorithm to determine the cutter posture at a point along any given direction, followed by an estimation method to evaluate the PCR along any given direction.

4.1 Determination of the cutter posture at a point along a cutting direction

To determine the cutter's posture at the point along an arbitrary cutting direction, the direct approach is to apply the CA algorithm to obtain the A-map first and then select a posture from it. However, due to the high computational complexity of the CA algorithm, we adopted a simple interpolation approach based on the A-maps of the sampled points. This is done by firstly finding a small neighborhood of $\mathbf{P}_c$ (e.g., 10–15 points) from the sampled points and selecting a cutter posture along the given cutting direction from their A-maps for each neighborhood point. Then, the result of the linear interpolation of these neighborhood postures is taken as the cutter posture at $\mathbf{P}_c$ along the given direction. Since the density of the sampled points is generally very high, linear interpolation should be able to achieve a reasonable approximation. The following discussion focuses on determining the cutter posture at a sampled point **P** along a given cutting direction from its A-map.

Within the A-map at **P**, an extensive number of cutter postures can be used to machine the local surface without interference. However, there exists one posture with which the cutter geometry at the point can closely match the part surface and produces the maximum machining strip width. Figure 3a shows the elliptical cross-section of the cutter on the normal plane perpendicular to a given cutting direction ***f***. The strip of the material that can be effectively removed by the cutter is determined from the cross-section and the surface with an offset of h (the desirable scallop height tolerance) from the part surface. It was suggested by Yoon et al. [23] that the machining strip width W decreases when the tilt angle λ is increased, as shown in Fig. 3b. Furthermore, W also decreases when $|\alpha|$ is increased since the cutter curvature increases at the point touching **P**, where α is the angle between the cutter axis direction **V** and cutting direction on $\boldsymbol{X}_L$–$\boldsymbol{Y}_L$ plane (see Fig. 3c). Based on this finding, a heuristic is adopted here to select a cutter posture such that W is maximized. From the A-map, we firstly find θ, which is the closest to the cutting direction angle in the local frame, and then take the minimum allowable λ from the A-map to form the posture (θ, λ) at **P**.

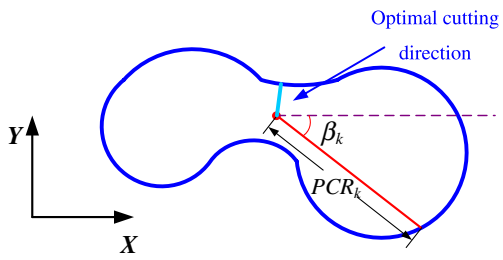

Fig. 2 The cutter S-map at a point on the part surface

4.2 Evaluation of PCR at a point along an arbitrary direction

A two-step procedure is developed to obtain the PCR at a point **P** along an arbitrary direction. In the first step, the discrete PCRs from the point to a number of neighboring sampled points are obtained. In the second step, a linear interpolation approach is adopted to calculate the PCR along any cutting direction.

In the first step, as shown in Fig. 4a, a local neighborhood of **P** is firstly defined that contains n sampled points $\{\mathbf{P}_j, j=1, 2\ldots n\}$, where n is the number of sampled points in the neighborhood. The neighborhood is formed based of distance of $\mathbf{PP}_j$, i.e., $|\mathbf{PP}_j| \le d_0$, where d_0 is a predefined value according to the curvature at $\mathbf{P}_i$. Intuitively, a small d_0 is preferred at the point with a large curvature, while a large d_0 at the point with a small curvature. Based on experiments, we take $d_0 = \min\{1/\max(|\kappa_{\max}|, |\kappa_{\min}|), XR\}$, where $\kappa_{\max}$ and $\kappa_{\min}$ are the principal curvatures, respectively, and R is the cutter major radius. Vector $\mathbf{PP}_j$ can be projected onto the ***X***–***Y*** plane, representing a discrete cutting direction β_j ($0° \le \beta_j \le 360°$). At the same time, cutter postures (θ, λ) at **P** and (θ_j, λ_j) at $\mathbf{P}_j$ along β_j are determined according to the method introduced in Section 4.1, and PCR_j is then calculated using Eq. 1.

In the second step, as shown in Fig. 4b, given an arbitrary cutting direction β in the global frame, we firstly find the two closest β_j to β from $\{PCR_j, j=1, 2, \ldots, n\}$. The PCR along β can then be obtained by applying linear interpolation of the two corresponding PCR_j.

5 Optimal tool-path generation

Up to now, the method for determining S-map at an arbitrary point has been established based on the A-maps of the sampled points. In this section, an optimization

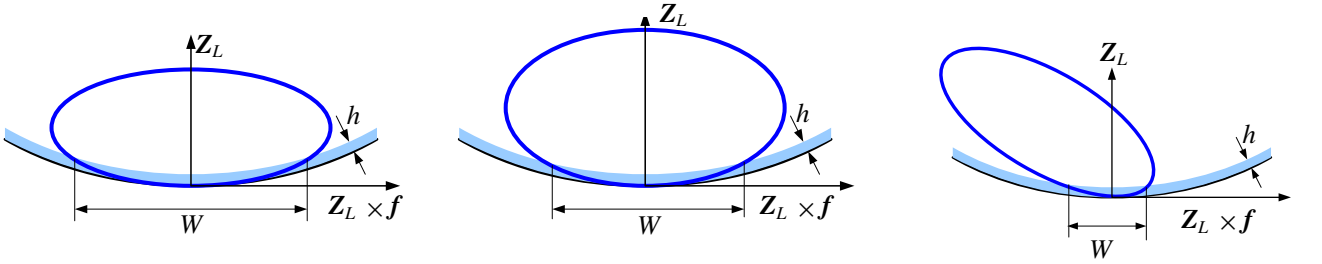

(a) cutter posture (α_0, λ_0) (b) cutter posture (α_0, λ_1), $\lambda_1 > \lambda_0$ (c) cutter posture (α_1, λ_0), $|\alpha_1| > |\alpha_0|$

Fig. 3 Machining strip width with different cutter postures. **a** Cutter posture (α_0, λ_0). **b** Cutter posture (α_0, λ_1), $\lambda_1 > \lambda_0$. **c** Cutter posture (α_1, λ_0), $|\alpha_1| > |\alpha_0|$

approach to generate tool-paths with minimum PCR at the CC points is introduced. The overall procedure involves two steps. In the first step, an initial tool-path is generated such that it follows the optimal cutting direction (with minimum PCR) at all CC points. In the second step, the adjacent tool-paths are generated in an iterative manner, one at a time, until the whole surface is covered.

5.1 Generation of the initial tool-path

The generation procedure starts with the identification of the first CC point, which is preferably on one of the surface boundaries (see Fig. 5a). This point is taken as the current CC point, $\mathbf{P}_i$. The S-map and the corresponding postures along each sampled feeding direction at $\mathbf{P}_i$ are then generated using the methods introduced in Section 4. The direction with the minimum PCR in the S-map of $\mathbf{P}_i$ is taken as the optimal cutting direction, $\boldsymbol{f}_i$, at $\mathbf{P}_i$ (see Fig. 5b). Along $\boldsymbol{f}_i$, the next CC point, $\mathbf{P}_{i+1}$, on the current path can be found such that the largest deviation d from the line segment $\mathbf{P}_i\mathbf{P}_{i+1}$ to the part surface is very close but less than the given surface error bound τ, as shown in Fig. 5c. Some reported solutions [5] can be employed for solving this problem. $\mathbf{P}_{i+1}$ becomes the current CC point and the cutting direction is determined following the same procedure as for $\mathbf{P}_i$. It is noted that based on this strategy for selecting the optimal cutting direction, there are cases that the current optimal direction varies significantly from the previous one. To ensure the smoothness of tool-path trajectory, the searching range for optimal cutting direction at the current CC point is limited to [−90°, 90°] from the previous optimal cutting direction. This process is repeated to find the next CC point and its optimal cutting direction until a boundary of the surface is reached. The initial tool-path is thus completely generated. This tool-path is considered as the current tool-path and is used to generate its adjacent tool-path.

5.2 Generation of the adjacent tool-path from the current one

The generation of the adjacent path to the current path involves two steps. In the first step, the CC points of the adjacent path are generated such that the machining efficiency is maximized. As shown in Fig. 6a, at a CC point $\mathrm{P}_j^i (j = 1, \ldots, n)$ of current path-i, where n is the total number of CC points, we can find the corresponding CC point P_j^{i+1} on the adjacent path-$(i+1)$ such that the maximum step-over size ΔW_j is achieved, i.e., the scallop height at P_j^i is close to but less than the scallop height tolerance h. This is done by firstly evaluating the machining strip widths (ω_{ai} and ω_{bi}) at P_j^i, which are the respective

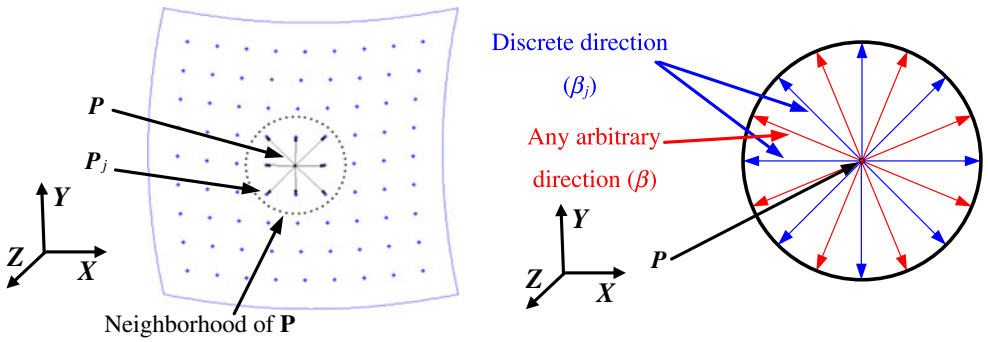

(a) PCR_j of the neighborhood of **P** (b) *PCR* at **P** along any directions

Fig. 4 Obtain the PCR at P along an arbitrary cutting direction. **a** PCR_j of the neighborhood of **P**. **b** PCR at **P** along any directions

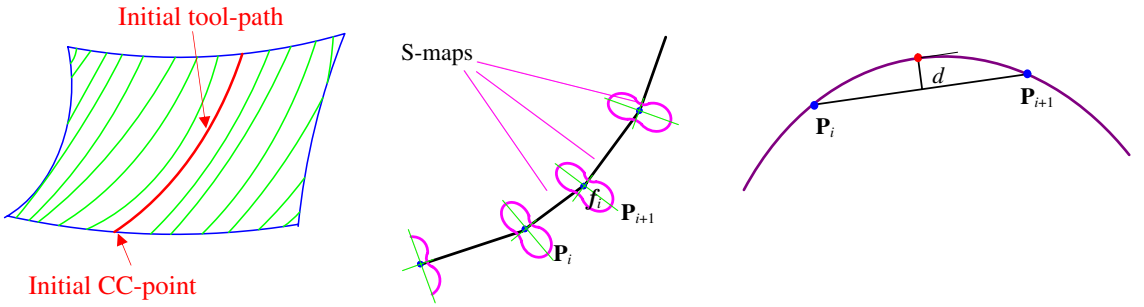

(a) The initial tool-path (b) The optimal cutting direction (c) Finding the next CC point along $\boldsymbol{f}_i$

Fig. 5 Generation of the initial tool-path. **a** The initial tool-path. **b** The optimal cutting direction. **c** Finding the next CC point along $\boldsymbol{f}_i$

distances from a CC point to the intersection points of cutter swept volume and the surface $\boldsymbol{S}_h$ with offset h from the part surface $\boldsymbol{S}$ (see Fig. 6b). The corresponding point P_j^{i+1} is then searched on the instantaneous plane such that the summation of corresponding ω ($w_{b,i}+w_{a,i+1}$ in Fig. 6c) is close to but greater than the distance of $\mathrm{P}_j^i\mathrm{P}_j^{i+1}$. In this search process, the cutter posture at a candidate P_j^{i+1} is determined using the method introduced in Section 4.1. The method proposed by Chiou and Lee [24] can be adopted here to evaluate the machining strip widths at a CC point. By linking the $\{\mathrm{P}_j^{i+1}\}$ using line segments, we obtain a path with high cutting efficiency. Since only the step-over size is maximized for the generation of $\{\mathrm{P}_j^{i+1}\}$ of this path, the resultant cutting direction and cutter posture may encounter sharp changes from one point to the other. This will certainly adversely affect the path smoothness. Therefore, we only take $\{\mathrm{P}_j^{i+1}\}$ as the candidate CC points of the adjacent path and apply some correction measures to adjust them to improve the path smoothness.

Since all the candidate CC points $\{\mathrm{P}_j^{i+1}\}$ are at positions with the maximum allowable step-over sizes, adjustment of these points effectively means reducing their step-over sizes and hence the machining efficiency will drop. To keep a decent level of machining efficiency, a constraint is adopted in the adjusting process, i.e., to ensure that the step-over size at any adjusted CC point is greater than a specific value. Here, the minimum step-over size among those at all the candidate CC points, i.e., $\Delta W_m=\min\{\Delta W_j\}, j=1, \ldots, n$, is taken as the lower bound of step-over size. Therefore, P_m^{i+1} will remain where it is and the remaining $\{\mathrm{P}_j^{i+1}\}$ are subjected to adjustment. Two heuristic-based algorithms are proposed to adjust the right hand (RH) points of P_m^{i+1}, i.e., $\{\mathrm{P}_k^{i+1}, k=m+1, \ldots, n\}$, and the left-hand (LH) points of P_m^{i+1}, i.e., $\{\mathrm{P}_k^{i+1}, k=m-1, \ldots, 1\}$, respectively, such that the minimum PCR is resulted. The following section will describe these two algorithms in details.

The RH-algorithm adjusts $\{\mathrm{P}_k^{i+1}, k=m+1, \ldots, n\}$ one at a time in a recursive manner, i.e., P_k^{i+1} (u_k, v_k) is adjusted based on P_{k-1}^{i+1}. The adjustment of P_k^{i+1} involves three steps as follows:

(1) As shown in Fig. 7a, starting from P_k^i, we find another corresponding CC point $\mathrm{P}'_k{}^{i+1}(u'_k, v'_k)$ with the minimum step-over size, ΔW_m. The cutting directions along $\mathrm{P}_{k-1}^{i+1}\mathrm{P}_k^{i+1}$ (β_k) and $\mathrm{P}_{k-1}^{i+1}\mathrm{P}'_k{}^{i+1}$ (β_k') are then calculated in global frame, respectively.
(2) Based on the S-map at P_{k-1}^{i+1}, the optimal cutting direction β_o is found in the range of $[\beta_k, \beta_k']$. In this step, we firstly uniformly sample the angular range of $[\beta_k, \beta_k']$ into a number of directions with each

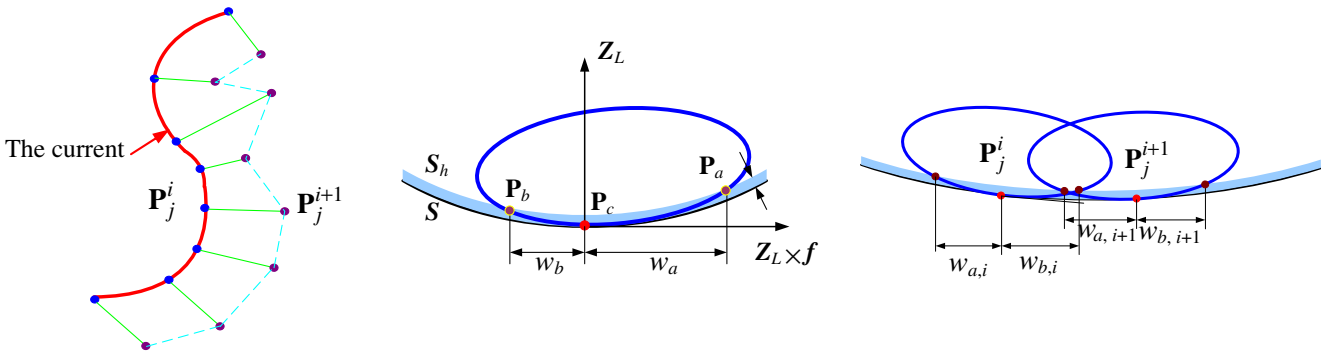

(a) The candidate CC point set (b) Machining strip width at a CC point (c) CC points on adjacent paths

Fig. 6 Candidate CC points of the adjacent path with maximum step-over size from the current one. **a** The candidate CC point set. **b** Machining strip width at a CC point. **c** CC points on adjacent paths

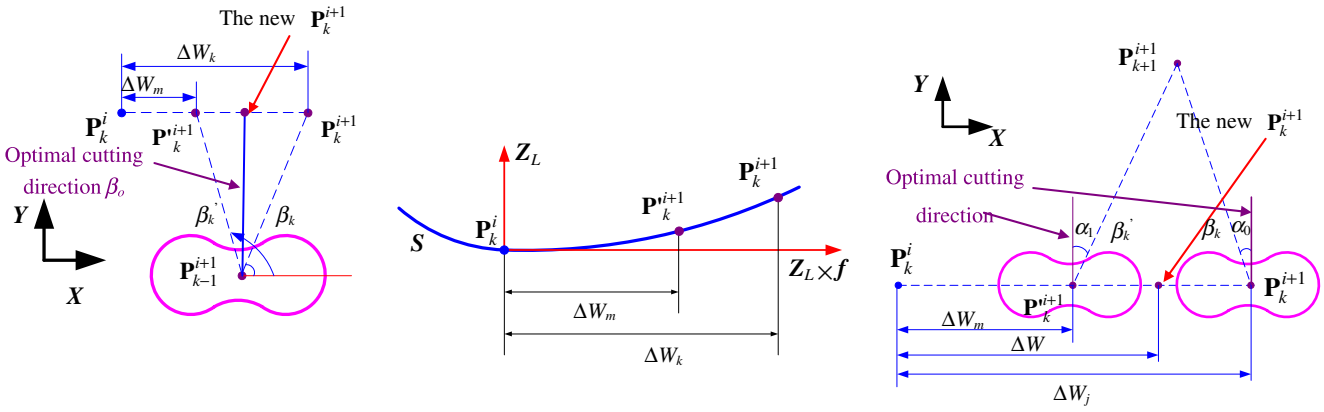

(a) Adjustment of a RH point (b) Searching for the corresponding points with different step-over sizes (c) Adjustment of a LH point

Fig. 7 Adjacent tool-path generation from the current one. **a** Adjustment of a RH point. **b** Searching for the corresponding points with different step-over sizes. **c** Adjustment of a LH point

direction corresponding to a discrete angle and calculate the PCR along each direction using the method described in Section 4.2. β_o is then taken as the discrete angle corresponding with the direction having the minimum PCR.

(3) The new P_k^{i+1} is obtained such that the cutting from P_{k-1}^{i+1} to the new P_k^{i+1} is along the optimal cutting direction β_o. In this step, the new P_k^{i+1} is searched as the surface point on the intersection of two planes, i.e., the instantaneous plane $\boldsymbol{Z}_L$–$\boldsymbol{Z}_L \times \boldsymbol{f}$ at P_k^i and the normal plane along β_o at P_{k-1}^{i+1}.

The LH-algorithm also adjusts $\{P_k^{i+1}, k=m-1, \ldots, 1\}$ one at a time in a recursive manner, i.e., P_k^{i+1} is adjusted based on P_{k+1}^{i+1}. The adjustment of P_k^{i+1} involves the following two steps:

(1) As shown in Fig. 7c, starting from P_k^i, we find another corresponding CC point $P_k'^{i+1}$ with the minimum step-over size, ΔW_m. The cutting directions along $P_k^{i+1}P_{k+1}^{i+1}$ (β_k) and $P_k'^{i+1}P_{k+1}^{i+1}$ (β_k') are then calculated in global frame, respectively.

(2) The optimal cutting direction towards P_{k+1}^{i+1} needs to be found so that the new P_k^{i+1} can be obtained. Unlike the RH-algorithm, in which the optimal cutting direction is found based on the S-map at the previous point, the LH-algorithm needs to consider the S-maps at all the points between $P_k'^{i+1}$ and P_k^{i+1}. This is because the S-map characterizes the dynamic property of cutter motion along its forward moving direction. With the consideration of relatively heavy computation of the S-map evaluation, we adopted a simple interpolation approach based on the S-maps only at P_k^{i+1} and $P_k'^{i+1}$. This is done by firstly obtaining the optimal cutting directions $\mathbf{V}_k$ at P_k^{i+1} and $\mathbf{V}_k'$ at $P_k'^{i+1}$, from their respective S-maps. The angular deviations α_0 (between β_k and $\mathbf{V}_k$) and α_1 (β_k' and $\mathbf{V}_k'$) are then evaluated. If α_0 and α_1 share the same sign, the new P_k^{i+1} is then taken from either P_k^{i+1} or $P_k'^{i+1}$, whichever has a smaller PCR. On the other hand, if α_0 and α_1 do not share the same sign, it means that there exists one point between $P_k'^{i+1}$ and P_k^{i+1} such that the optimal direction found from its S-map is coincident with the direction pointing to P_{k+1}^{i+1}. A new step-over size ΔW is estimated using the following interpolation equation:

$$\Delta W = \Delta W_m + \frac{|\alpha_1|}{|\alpha_0| + |\alpha_1|}(\Delta W_k - \Delta W_m) \tag{2}$$

The new P_k^{i+1} is then obtained such that the step-over size is ΔW. Since the machined surface is generally well-behaved and the original P_k^{i+1} and $P_k'i+1$ are relatively close, the similarity of the surface properties around these two points must be very high. Therefore, the interpolation approach should be able to achieve a reasonable approximation.

5.3 The overall algorithm

Combining the above algorithms for generating the initial tool-path and the adjacent tool-paths (one at a time), the overall algorithm for optimal tool-path generation with smooth cutter posture change and high cutting efficiency is given as follows:

Algorithm: Generating optimal tool-paths for five-axis sculptured surface finish milling
Input: (1) A NURBS surface $S(u, v)$
(2) A fillet-end cutter (R, r_f, L)
(3) Machining profile tolerance τ and h

(4) A-maps at all sampled points

Output: Tool-paths with a set of CC points (including their postures)

Begin

(1) Set the tool-path set {TPS}={Φ} and CC points set {$\mathbf{P}_{cc}$}={Φ}.

(2) Find the initial tool-path (ITP) and the CC points, using the algorithm introduced in Section 5.1. Put ITP into {TPS}, and the CC points into {$\mathbf{P}_{cc}$}.

(3) Generate the adjacent tool-paths from the right side of ITP.

(a) Set ITP as the current Path-i.

(b) Put all the CC points on Path-i into a set {P_j^i}, j =1, …, n.

(c) Find all the corresponding CC points {P_j^{i+1}}, j =1, …, n, such that the step-over size is maximized with the desirable h. Take {P_j^{i+1}} as the candidate points. If all {P_j^{i+1}} are beyond the surface boundary, go to (4).

(d) Correct the candidate points {P_j^{i+1}}, j =1, …, n on path-(i+1)

(i) Find the minimum ΔW_m from those at {P_j^{i+1}}, j =1, …, n.

(ii) Starting from P_m^{i+1}, adjust {P_k^{i+1}, k=m+1, …, n} one at a time in a recursive manner, i.e., P_k^{i+1} is adjusted based on P_{k-1}^{i+1}, using the RH-algorithm.

(iii) Starting from P_m^{i+1}, adjust {P_k^{i+1}, k=m-1, …, 1} one at a time in a recursive manner, i.e., P_k^{i+1} is adjusted based on P_{k+1}^{i+1}, using the LH-algorithm.

(e) Put the newly generated path into {TPS} and CC points into {$\mathbf{P}_{cc}$}. Set i=i+1, go to (b).

(4) Generate the adjacent tool-paths from left side of ITP, using a similar algorithm to (3).

(5) Output {$\mathbf{P}_{cc}$} and {TPS}.

End

It is worth noting that during the generation of CC points on the adjacent tool-path, the scallop height between the current tool-path and the adjacent one is kept within the specified tolerance. There is no control mechanism for the profile error between the newly generated tool-path and the part surface. This may lead to two problems. Firstly, the step-forward size between two neighboring CC points is too large, leading to the profile error out of the tolerance. Secondly, the step-forward size is too small, which may result in much complexity in the subsequent adjacent tool-paths (e.g., sudden change of feeding direction). Therefore, a correction process is applied to the newly generated CC points in the current implementation. Firstly, we map all the CC points onto the (u, v) frame and link them using line segments. The (u, v) frame is the parametric frame for a NURBS surface. Its counterpart is the (X, Y, Z) frame in the Cartesian space. Their relationship can be described as$(X, Y, Z) = S(u, v)$. Secondly, the CC points are relocated along these linear segments such that the step-forward size has the maximum allowable value subject to the profile error tolerance. In this correction process, the total number of CC points may change. It is expected that the machining efficiency is maximized while the surface accuracy is maintained.

In this paper, the cutter posture change is evaluated in the global frame without considering the machine configuration. Therefore, the smoothness of the generated tool-paths is true only when the change in the cutter posture is proportional to the change of the joint angles in general. We believe that this condition is generally satisfied when the cutter posture is reached well within the reachable space of the joint angles. However, the joint angles can be very different for two similar cutter postures when they are near the boundary of reachable space. To resolve this problem, one possible solution is to represent the A-maps in terms of joint angles and remove the range near the boundary of reachable space before tool-path generation.

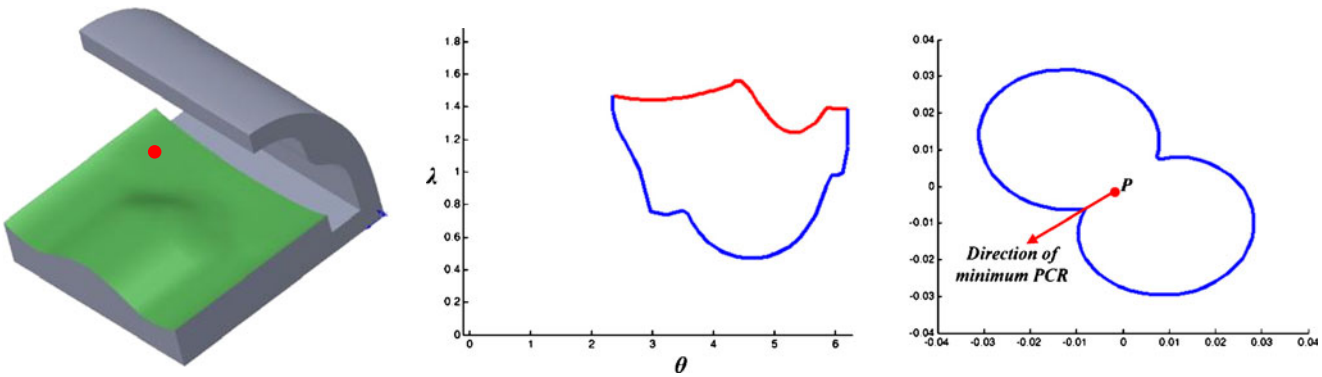

(a) The example part (b) The A-map at (u=0.2, v=0.8) (c) The S-map at (u=0.2, v=0.8)

Fig. 8 The example part surface with information of A-map and S-map. **a** The example part. **b** The A-map at (u=0.2, v=0.8). **c** The S-map at (u=0.2, v=0.8)

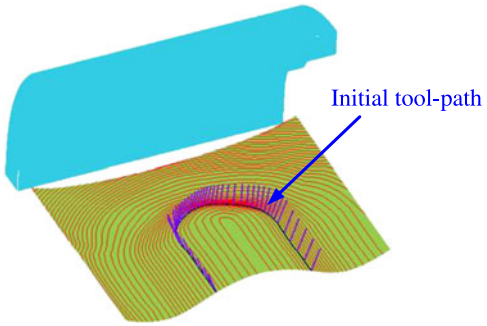

(a) Optimal tool-paths (the proposed method)

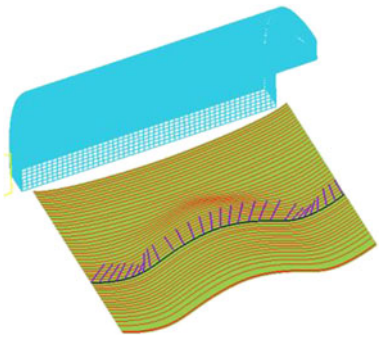

(b) Optimal tool-path (iso-planar method)

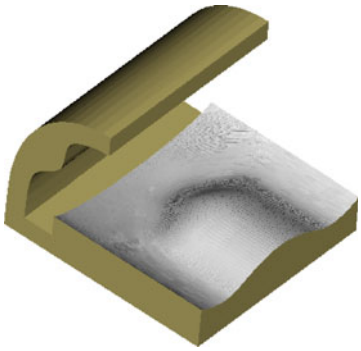

(c) Machining simulation (the proposed method)

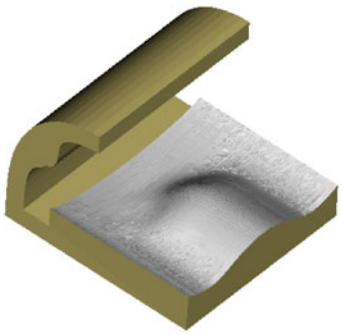

(d) Machining simulation (iso-planar method)

Fig. 9 Optimal tool-path generation with the proposed method and the iso-planar method. **a** Optimal tool-paths (the proposed method). **b** Optimal tool-path (iso-planar method). **c** Machining simulation (the proposed method). **d** Machining simulation (iso-planar method)

6 An application example and discussion

The proposed method has been implemented using C++ and OpenGL. In this section, an example for optimal tool-path generation to machine (finishing cut) a sculptured surface is firstly presented to demonstrate the efficacy of the developed method. Furthermore, a comparison is conducted between the proposed method and a similar optimization method based on iso-planar cutting pattern.

Figure 8a shows an example part surface of a chair seat (similar to the example used in [18]), which consists of concave, convex, and saddle regions. To test our algorithm's ability for global interference avoidance, an arch-shaped overhang was also added to provide some non-machining obstacle surfaces. The machining surface was sampled uniformly along u and v directions into 201×201 points. A fillet-end cutter T(R, r_f)=(6 mm, 0.5 mm) was selected to mill this surface. The A-maps of the cutter at every sampled point were then obtained. Figure 8b shows the A-map at a surface sampled point (u=0.2, v=0.8). Based on these A-maps, the S-map at any arbitrary point can be evaluated, using the algorithms introduced in Section 4. Figure 8c shows the S-map at a point (u=0.2, v=0.8). The direction of 206.3° from ***X***-axis has the minimum PCR (0.0092 mm^{-1}), while the direction of 123° from the ***X***-axis has the maximum PCR (0.0362 mm^{-1}).

Both the profile error tolerance and the scallop height tolerance were set to be 0.1 mm. The proposed method was firstly used for tool-path generation. The generated tool-path is shown in Fig. 9a in which the initial path is indicated in black and the cutter's postures at some CC points are displayed. It can be seen that the posture changes over the whole path are very small. For comparison, another optimal tool-path method based on iso-planar path pattern developed earlier [25] was also used to generate the tool-path for this surface using the same cutter. The iso-planar based method also considers both path smoothness

Table 1 A comparison of the generated paths (proposed method vs. iso-planar method)

Algorithm	Number of passes	Number of CC points	Total path length (mm)	Average PCR (mm^{-1})
The proposed method	57	1,524	3,528.2	0.0108
The iso-planar method	62	3,106	6,415.7	0.0459

and cutting efficiency. It firstly selects the optimal cutting direction along which the average PCR of all the sample points is minimized and then generates the tool-path, one at a time, such that the step-over size between the neighboring paths is maximized. The generated iso-planar tool-path is shown in Fig. 9b, as well as the cutter's postures at some CC points on one path. To validate the quality of the tool-paths generated using these two methods, machining simulation experiments of the example part were conducted in the VERICUT® environment and the resulted machined surfaces are shown in Fig. 9c and d, respectively. The AUTODIFF module in the VERICUT® was then used for direct graphic simulation to check gouging and surface error of the generated tool-paths. In both cases, the machining errors are limited within the specified tolerance.

Table 1 summarizes the evaluation results of these two generated tool-paths under different criteria. It can be seen that the path based on the proposed method has fewer passes and CC points than the iso-planar path. More importantly, the former has a much shorter overall length than the iso-planar path, though maximized cutting efficiency is set as target in both methods. As for the average PCR (the summation of all the posture changes from one CC point to another/path length) over the whole path, the path based on the proposed method is much smoother than the iso-planar path (0.0108 vs. 0.0459). Therefore, it is concluded that in this case study, the proposed method outperforms the iso-planar method significantly based on both path smoothness and machining efficiency.

In the proposed method, although tool-path smoothness is the first priority during tool-path generation, it is noted in the case study that on the propagated tool-paths that are far away from the initial path, the cutter postures along the resultant feeding directions might not be globally smooth, especially when the shape of the part surface changes drastically from one region to the other. This is due to the correction process for achieving error control and reasonable machining efficiency. One alternative to resolve this problem, to a certain extent, is to follow a similar approach to [18] by generating several initial tool-paths spreading over the part surface and then obtain the adjacent tool-paths in relatively smaller regions, respectively. However, complication may arise when the propagated tool-paths from different initial tool-paths meet. Therefore, the current implementation with a single initial tool-path provides a relatively balanced and stable solution.

7 Conclusions

This paper presents a new method for generating five-axis tool-paths with smooth tool motion and high efficiency based on the accessibility map (A-map) of the cutter at a point on the part surface. A cutter smoothness map called the S-map, which characterizes posture change rates along all the possible cutting directions at a point is constructed based on the A-map of the cutter. Based on the A-maps and S-maps of all the sampled points of the part surface, an iterative searching algorithm has been developed to generate tool-paths for five-axis sculptured surface machining (finish cut). In the algorithm, the path smoothness is considered as the top priority while machining efficiency the second. Compared with the traditional tool-path generation methods, e.g., iso-planar, the developed method can generate tool-paths to achieve smaller cutter posture change over the entire path and shorter overall too-path length. The developed techniques can be used to automate the five-axis tool-path generation, in particular for high speed machining.

Acknowledgments The work reported in this paper has been supported by A*STAR of Singapore under the project R265-000-176-305.

References

1. Balasubramaniam M, Sarma SE, Marciniak K (2003) Collision-free finishing toolpaths from visibility data. Comput-Aided Des 35:359–374
2. Morishige K, Takeuchi Y, Kase K (1999) Tool path generation using C-space for 5-axis control machining. ASME J Manuf Sci Eng 121:144–149
3. Wang N, Tang K (2007) Automatic generation of gouge-free and angular-velocity-compliant five-axis tool path. Comput-Aided Des 39:841–852
4. Makhanov SS (2009) Adaptable geometric patterns for five-axis machining: a survey. Int J Adv Manuf Tech 47:1167–1208
5. Choi BK, Park JW, Jun CS (1993) Cutter-location data optimization in 5-axis surface machining. Comput-Aided Des 25:377–386
6. Li SX, Jerard RB (1994) Five-axis machining of sculptured surfaces with a flat-end cutter. Comput-Aided Des 26:165–178
7. Kiswanto G, Lauwers B, Kruth JP (2007) Gouging elimination through tool lifting in tool path generation for five-axis milling based on faceted models. Int J Adv Manuf Tech 32:293–309
8. Elber G, Cohen E (1994) Tool path generation for freeform surface models. Comput-Aided Des 26:490–496
9. Sun YW, Guo DM, Jia ZY, Wang HX (2006) Iso-parametric tool path generation from triangular meshes for free-form surface machining. Int J Adv Manuf Tech 28:721–726
10. Kim T (2007) Constant cusp height tool paths as geodesic parallels on an abstract Riemannian manifold. Comput-Aided Des 39:477–489
11. Li H, Feng FY (2004) Efficient five-axis machining of free-form surfaces with constant scallop height tool-paths. Int J Prod Res 43:2403–2417
12. Lo CC (1999) Efficient cutter-path planning for five-axis surface machining with a flat-end cutter. Comput-Aided Des 31:557–566
13. Tournier C, Duc E (2005) Iso-scallop toolpath generation in 5-axis milling. Int J Adv Manuf Tech 25:867–875
14. Park SC, Choi BK (2000) Tool-path planning for direction-parallel area milling. Comput-Aided Des 32:17–25

15. Wang HP, Chang H, Wysk RA, Chandrawarkar A (1987) On the efficiency of NC tool-path planning for face milling operations. ASME, J Eng Ind 109:370–376
16. Kruth JP, Klewais P (1994) Optimization and dynamic adaptation of the cutter inclination during five-axis milling of sculptured surfaces. CIRP Ann 43:443–448
17. Kim T, Sarma SE (2002) Toolpath generation along directions of maximum kinematic performance; a first cut at machine-optimal paths. Comput-Aided Des 34:453–468
18. Chiou CJ, Lee YS (1999) A shape-generating approach for multi-axis machining G-buffer models. Comput-Aided Des 31:761–776
19. López de Lacalle LN, Lamikiz A, Sánchez JA, Fernádez de Bustors I (2006) Recording of real cutting forces along the milling of complex parts. Mechatron 16:21–32
20. López de Lacalle LN, Lamikiz A, Sánchez JA, Salgado MA (2007) Toolpath selection based on the minimum deflection cutting forces in the programming of complex surfaces milling. Int J Mach Tools Manuf 47:388–400
21. O'Neil B (1966) Elementary differential geometry. Academic, New York
22. Li LL, Zhang YF (2006) Cutter selection for 5-axis milling of sculptured surfaces based on accessibility analysis. Int J Prod Res 44:3303–3323
23. Yoon JH, Pottmann H, Lee YS (2003) Locally optimal cutting positions for 5-axis sculptured surface machining. Comput-Aided Des 35:69–81
24. Chiou CJ, Lee YS (2002) A machining potential field approach to tool-path generation for multi-axis sculptured surface machining. Comput-Aided Des 34:357–371
25. Li LL, Zhang YF (2006) An integrated approach towards process planning for 5-axis milling of sculptured surfaces. Comput-Aided Des Appl 3:249–258